Electronic Supplementary Material (ESI) for ChemComm.
This journal is © The Royal Society of Chemistry 2021

Electronic Supplementary Information (ESI)

Engineering Fe_2O_3/FeS hybrid catalyst from a deep eutectic solvent for highly efficient electrocatalytic N_2 fixation

Tingting Chen, Hao Ying, Chenyun Zhang, Jiahui Bi, Zhonghao Li*, Jingcheng Hao

Key Laboratory of Colloid and Interface Chemistry, Ministry of Education, Shandong University, Jinan, 250100, P. R. China, E-mail: zhonghaoli@sdu.edu.cn

Experimental Section

Materials and Chemicals.

Choline chloride (ChCl), sodium hypochlorite solution (NaClO) and sodium nitroferricyanide dihydrate ($C_5FeN_6Na_2O \cdot 2H_2O$) were bought from Shanghai Macklin Biochemical Co., Ltd. Thiourea (H_2NCSNH_2), sodium citrate dehydrate ($C_6H_5Na_3O_7 \cdot 2H_2O$), ammonium chloride ($NH_4Cl$) and urea ($H_2NCONH_2$) were obtained from Sinopharm Chemical Reagent Co., Ltd. Fe foam was supplied by Kunshan Longshengbao Electronic Materials Co., Ltd. Salicylic acid ($C_7H_6O_3$), para-(dimethylamino) benzaldehyde (p-$C_9H_{11}NO$) and hydrazine monohydrate ($N_2H_4 \cdot H_2O$) were obtained from Aladdin Chemistry Co., Ltd. 5 wt% nafion solution was purchased from the Sigma Co., Ltd. Carbon cloth was obtained from Changsha Lyrun Material Co., Ltd. Nafion 211 membrane was purchased from Wuhan GaossUnion technology Co., Ltd.

Preparation of the choline chloride (ChCl)/thiourea DES.

ChCl/thiourea DES was synthesized via mixing the ChCl (3.630 g, 0.026 mol) and thiourea (3.958 g, 0.052 mol) with vigorous stirring in an oil bath of 80 °C based on the reported procedure. [1] The DES was formed until a clear liquid appeared.

Ionothermal synthesis of FeS in DES.

Prior to preparing the catalyst, Fe foam with the area of 1 × 3 cm^2 (0.35 g) was pretreated by sonication in acetone and ethanol for about 10 min and then dried in a vacuum oven. As for the synthesis of FeS, the treated Fe foam was immersed in as-prepared ChCl/thiourea DES (7.5 g) in a teflon-lined stainless autoclave. During the

process of heating at 180 °C for 12 h in an oven, the Fe foam was reacted thoroughly with the DES. The product was recovered by centrifugation and washed by ethanol and water. Finally, the sample was dried in vacuum at room temperature for further use.

Synthesis of hybrid of crystalline Fe_2O_3 with amorphous FeS (Fe_2O_3/FeS).

The above as-obtained FeS of 20 mg was taken out and put into a tube furnace in air atmosphere. The temperature of the furnace was raised with a rate of 5 °C min^{-1} and kept at 400 °C for 2 h. The prepared sample was cooled to the room temperature, then washed with ethanol and water and finally dried in vacuum.

Synthesis of Fe_2O_3.

ChCl/urea DES was prepared via mixing the ChCl (3.630 g, 0.026 mol) and urea (3.123 g, 0.052 mol) with vigorous stirring at 80 °C. Then the synthesis process of Fe_2O_3 was similar to that of synthesizing FeS except for using the ChCl/urea DES as solvent. After the ionothermal process, the product was collected from Fe foam surface by ultrasound in ethanol and water and finally dried in vacuum.

Material Characterizations.

Transmission electron microscopy (TEM) and high-resolution transmission electron microscopy (HRTEM) images were observed from a talos F200X microscope. X-ray diffraction (XRD) data were collected from the Rigaku Dmax-rc X-ray diffractometer. X-ray photoelectron spectroscopy (XPS) characterization was measured on the X-ray photoelectron spectrometer (ESCALAB 250 XI). Energy-dispersive X-ray (EDX) elemental mapping images were obtained from Oxford-

instruments XMaxN. ^1H nuclear magnetic resonance (NMR) characterization was conducted on a Bruker Avance 400 spectrometer. The specific surface area was characterized by N_2 adsorption-desorption measurement on micromeritics ASAP 2460. The absorption spectra were carried out on a Shimadzu UV-2600 UV-Vis spectrophotometer.

Electrochemical Measurements.

The electrochemical tests were conducted on the gastight H-type cell with CHI 760E electrochemical workstation using the three-electrode system that contained saturated Ag/AgCl reference electrode and Pt sheet counter electrode. The working electrode was carbon cloth modified with catalyst. The modification procedures were as follows. Catalyst ink was firstly prepared by suspending 5 mg sample in a mixed solution of 480 μL absolute ethanol, 480 μL water and 40 μL 5 wt% Nafion solution with 1 h sonication. Then a carbon cloth of 1 × 1 cm^2 was loaded with the 30 μL homogeneous ink and dried in vacuum oven. The Nafion 211 membrane used to separate the H-type cell was pretreated by incubation in boiling water and 5% H_2O_2 solution for 1 h at 80 ^oC. After soaking in the 0.5 M H_2SO_4 for 3 h, the preconditioned membrane was finally processed in the water for 6 h at 80 ^oC. For electrochemical characterization test, cathodic compartment of the cell was filled with N_2-saturated electrolyte achieved by purging pure N_2 for 30 min to remove residual air before measurement. Before the NRR electrolysis, the feeding gas was purified by passing through the acid trap (H_2SO_4, 0.05 M). To probe NRR activity of the synthesized catalysts preliminarily, linear sweep voltammetry (LSV) test with 5 mV s^{-1} was

conducted from -0.1 V to -0.4 V. Double-layer capacitance (C_{dl}) was carried out to reflect electrochemically active surface area (ECSA) from cyclic voltammetry (CV) experiments between 0.2 V to 0.3 V with various scanning rates. There was no faradaic current response in the potential range. Capacitive current at 0.25 V ($\Delta J = J_a - J_c$) was done against scan rate, in which the linear slope was twice of C_{dl}. Electrochemical impedance spectroscopy (EIS) characterization was conducted at 5 mV in frequency range of 0.1 to 10^6 Hz. The electrochemical measurements were done at room temperature. The potentials mentioned were standardized into reversible hydrogen electrode (RHE) scale via following equation:

$$E_{RHE} = E_{Ag/AgCl} + 0.059 \times pH + 0.197 \text{ V}$$

(1)

Determination of Ammonia.

The amount of NH_3 during electrolysis was spectrophotometrically measured using a colorimetric indophenol blue method.[2] Briefly, 2 mL cathodic electrolyte or solution in absorber was transferred into a tube after NRR and mixed thoroughly with 2 mL NaOH solution (1 M) involving 5 wt% sodium citrate and 5 wt% salicylic acid, 1 mL NaClO (0.05 M) as well as 0.2 mL sodium nitroferricyanide solution (1 wt%) in turn. After 2 h color development in dark, the mixture was analyzed with the absorbance at 655 nm. The concentrations of NH_3 were estimated from standard concentration-absorbance curve plotted by measuring absorbance of NH_4Cl solution with different concentration (0.0, 0.1, 0.2, 0.4, 0.6, 0.8, 1.0, 1.5 μg mL^{-1}). Then the NH_3 yield and Faradaic efficiency (FE) were achieved according to the following

equations. For FE, the ratio of charge amount for NRR to total charge in the whole electrolysis process, was then calculated with the assumption of one NH_3 molecule consuming three electrons.

$$r_{NH_3} = (C_{NH_3} \times V) / (t \times m_{cat.}) \quad (2)$$

$$FE = (3F \times C_{NH_3} \times V) / (17 \times Q)$$

(3)

Here C_{NH_3} was the tested NH_3 concentration, V meant the electrolyte volume in cathodic cell or solution in absorber for NH_3 collection, t was the electeoreduction time, $m_{cat.}$ represented the catalyst mass loading on a carbon cloth, F was the Faraday constant of 96485 C mol^{-1}, Q was quantity of the charge passing electrode in whole reaction.

Determination of Hydrazine.

N_2H_4 was detected by the Watt and Chrisp method,[3] in which color reagent was obtained via mixing 0.599 g p-$C_9H_{11}NO$, 3 mL of concentrated HCl and 30 mL of ethanol. In detail, 5 mL cathodic electrolyte or solution in the absorber was taken out, followed by mixing with 5 mL color reagent and then standing 10 min. Finally, the absorbance of the resulted solution was determined at 455 nm. The calibration curve was obtained by adding color reagent to standard N_2H_4 solutions with known concentration as 0, 0.1, 0.5, 1, 1.5, 2.0 μg mL^{-1} separately.

^{15}N isotope labeled experiment.

We defined the origination of detected NH_3 by using $^{15}N_2$ gas instead of $^{14}N_2$ as the feeding gas, and performed the ^1H NMR spectroscopy on Bruker Avance

spectrometer.

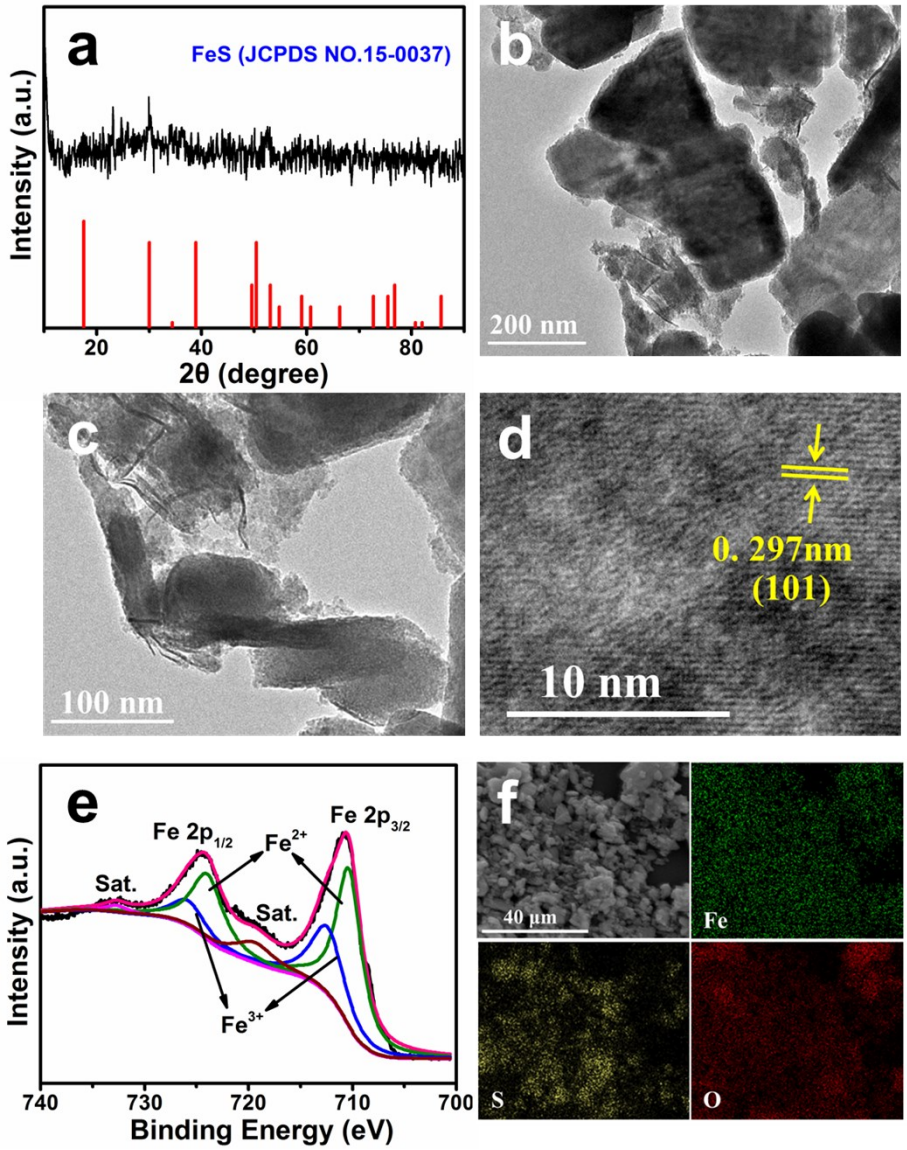

Fig. S1 Characterizations of the as-prepared FeS from ionothermal reaction. (a) XRD pattern, (b) low- and (c) high-magnification TEM image, (d) HRTEM image, (e) Fe 2p high-resolution XPS spectrum, (f) EDX elemental mapping images.

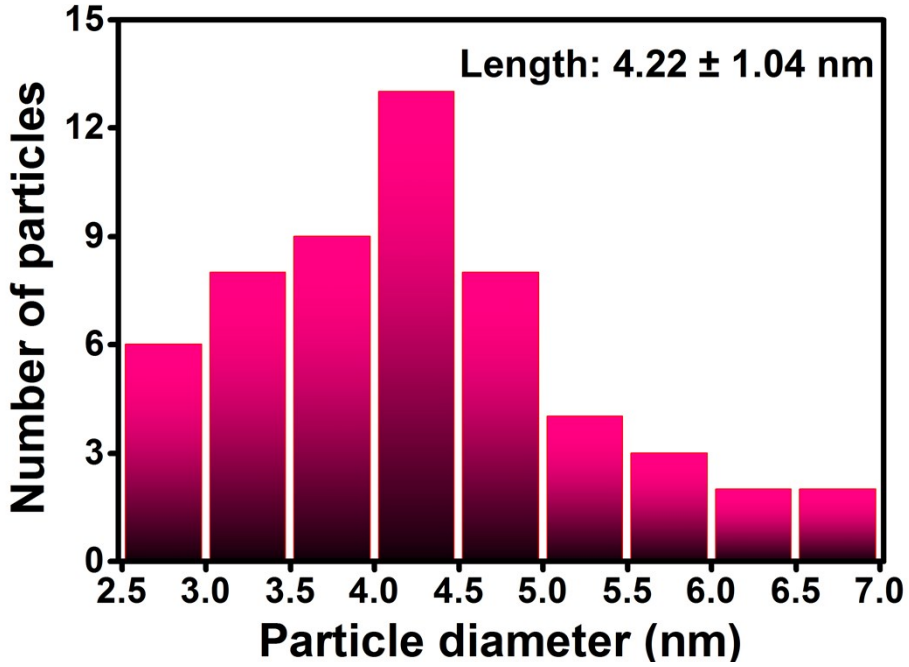

Fig. S2 Particle size distribution of nanoparticle subunits of FeS particles.

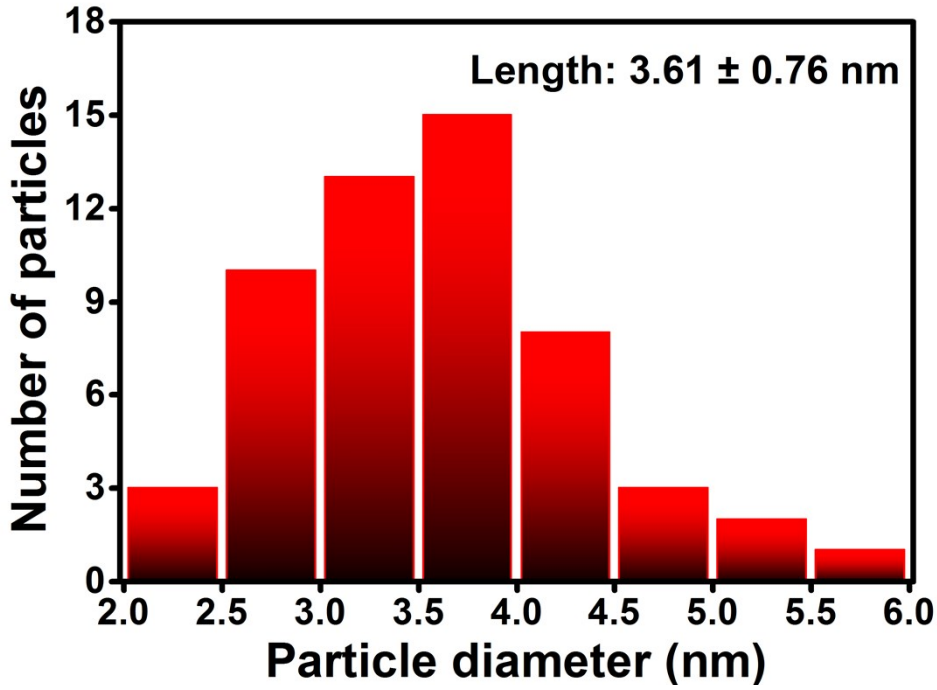

Fig. S3 Particle size distribution of nanoparticle subunits of Fe_2O_3/FeS particles.

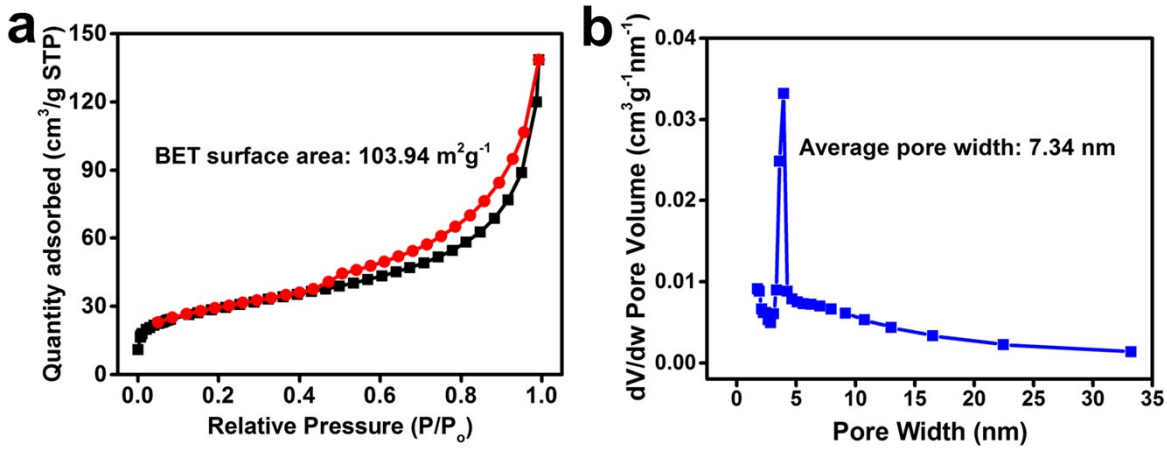

Fig. S4 (a) Nitrogen adsorption-desorption isotherms, (b) pore-size distributions of Fe_2O_3/FeS.

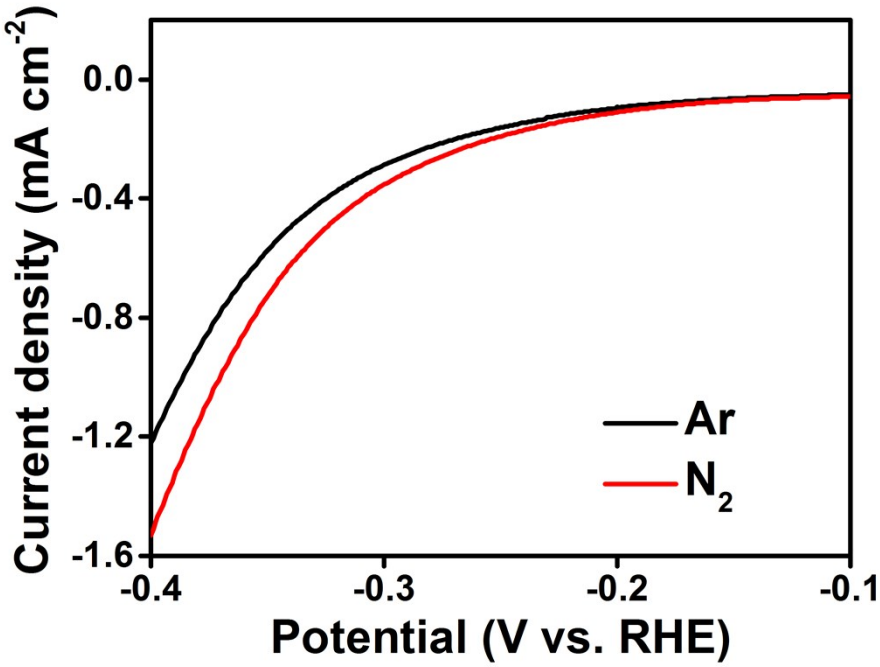

Fig. S5 LSV curves of Fe_2O_3/FeS in N_2- and Ar-saturated 0.1 M KOH electrolyte.

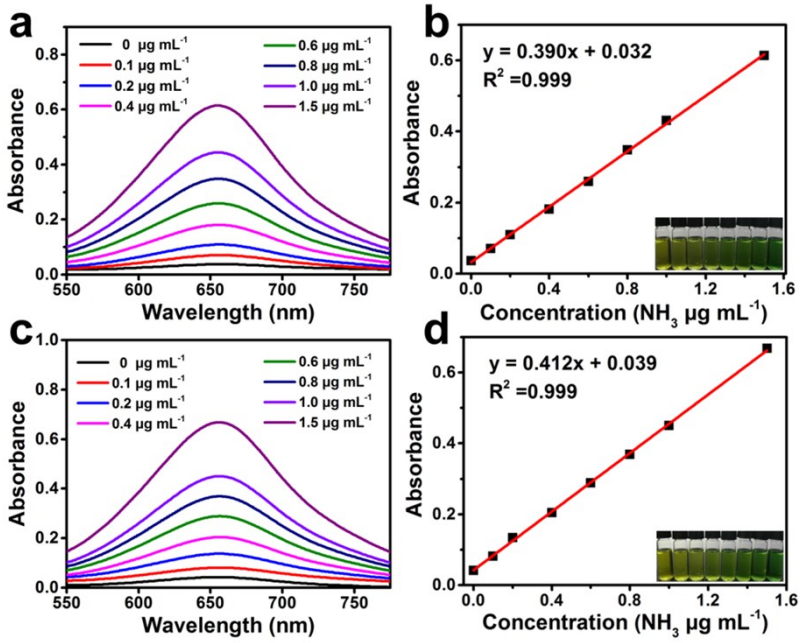

Fig. S6 The quantification of NH_3 using indophenol blue method. UV-Vis absorption spectra and calibration curve of NH_4Cl solutions with different concentration colored indophenol assays. (a) and (b) 0.1 M KOH, (c) and (d) 0.001 M H_2SO_4。

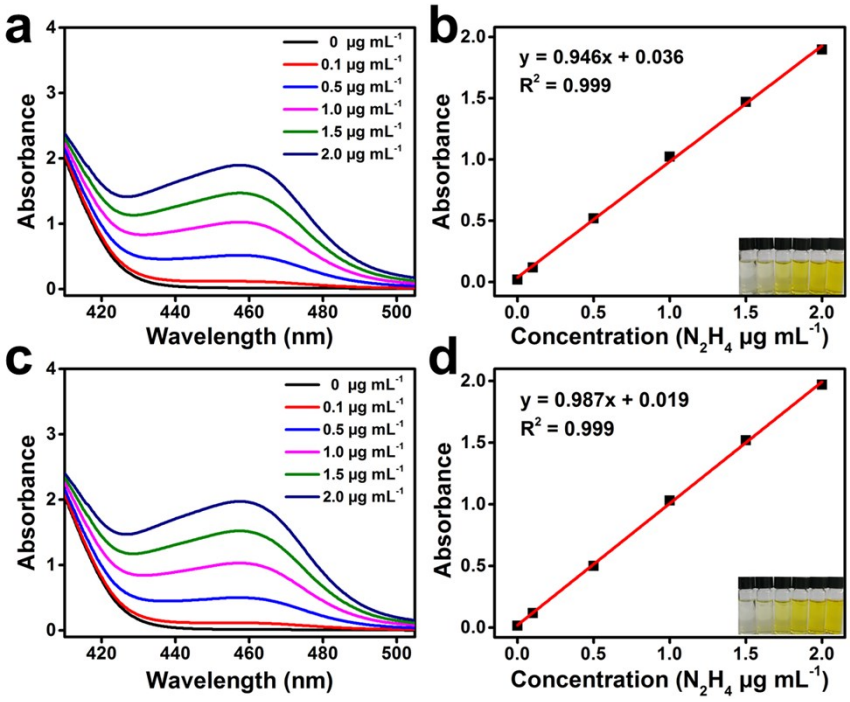

Fig. S7 UV-Vis absorption spectra and calibration curve of N_2H_4 colorimetric assays using Watt-Chrisp method. (a) and (b) 0.1 M KOH, (c) and (d) 0.001 M H_2SO_4。

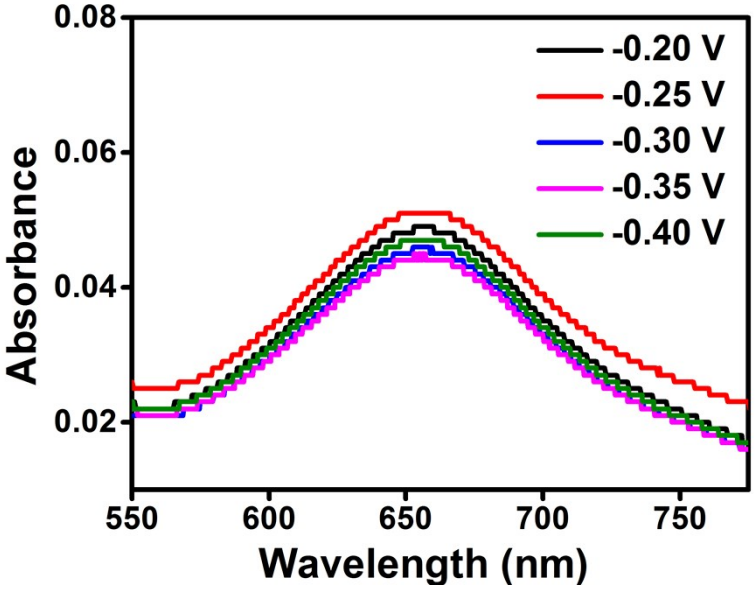

Fig. S8 UV-Vis absorption spectra of solutions from absorber colored with indophenol indicator under the selected potentials.

Table S1. NH_3 yields and Faradaic efficiencies of Fe_2O_3/FeS particles at the given potentials.

Potential (V vs. RHE)	**NH_3 yield ($\mu g\ h^{-1}\ mg_{cat.}^{-1}$)**	**Faradaic efficiency (%)**
-0.20	23.74	24.70
-0.25	34.31	18.06
-0.30	28.25	7.04
-0.35	27.24	2.52
-0.40	29.59	1.03

Table S2. Comparison of NH_3 yield and Faradaic efficiencies with state-of-the-art NRR electrocatalysts reported recently.

Catalyst	Potential (V vs. RHE)	NH_3 yield	FE (%)	Ref.
p-Fe_2O_3/CC	-0.4	13.56 μg h^{-1} $mg_{cat.}^{-1}$	7.69	4
Fe_2O_3/Cu	-0.1	15.66 μg h^{-1} $mg_{cat.}^{-1}$	24.4	5
Fe_2O_3/CP	-0.8	15.9 μg h^{-1} $mg_{cat.}^{-1}$	0.94	6
FeS_2	-0.5	37.2 μg h^{-1} $mg_{cat.}^{-1}$	11.2	7
Fe_3C@C	-0.2	8.53 μg h^{-1} $mg_{cat.}^{-1}$	9.15	8
Au-Fe_3O_4	-0.2	21.42 μg $mg_{cat.}^{-1}$ h^{-1}	10.54	9
Fe-N/C-CNTs	-0.2	34.83 μg h^{-1} $mg_{cat.}^{-1}$	9.28	10
1T-MoS_2/g-C_3N_4	-0.3	29.97 μg h^{-1} $mg_{cat.}^{-1}$	20.48	11
BP QDs/MnO_2	-0.5	25.3 μg h^{-1} $mg_{cat.}^{-1}$	6.7	12
Ni_2P/N-C	-0.2	34.4 μg h^{-1} $mg_{N2P.}^{-1}$	17.21	13
CrN NCs	-0.5	31.11 μg h^{-1} $mg_{cat.}^{-1}$	16.6	14
$Bi_4V_2O_{11}$/CeO_2	-0.2	23.21 μg h^{-1} $mg_{cat.}^{-1}$	10.16	15
WO_3-40kGy	-0.3	4.9 μg $mg_{cat.}^{-1}$ h^{-1}	23	16
NiTe	-0.1	33.34 ±0.70 μg h^{-1} mg^{-1}	17.38 ±0.36	17
Sn/SnS_2	-0.8	23.8 μg h^{-1} mg^{-1}	6.5 (-0.7 V)	18
Fe_2O_3/FeS	**-0.25**	**34.31 μg h^{-1} $mg_{cat.}^{-1}$**	**18.06**	**This work**

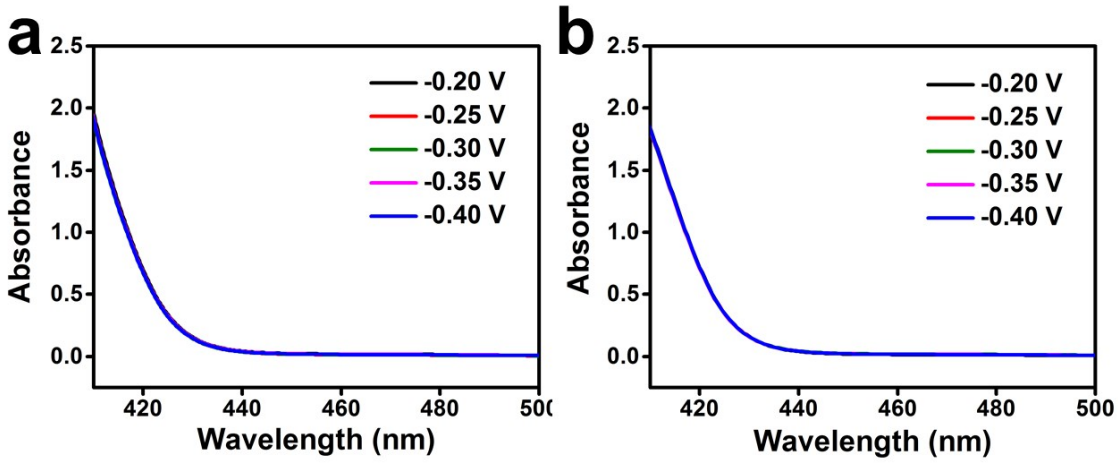

Fig. S9 UV-Vis absorption spectra of N_2H_4 detection after 2 h electrolysis at selected potentials with Watt-Chrisp method. (a) cathodic electrolytes, (b) corresponding solutions obtained from absorber.

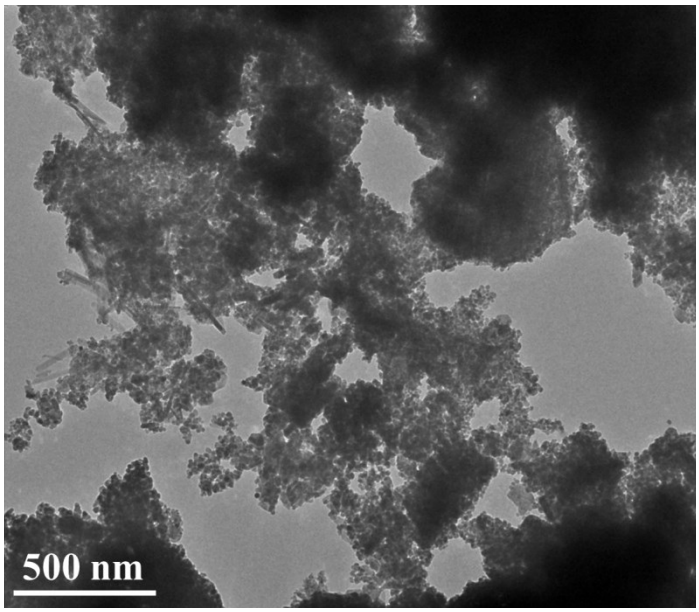

Fig. S10 TEM image of catalyst after long-term electrolysis.

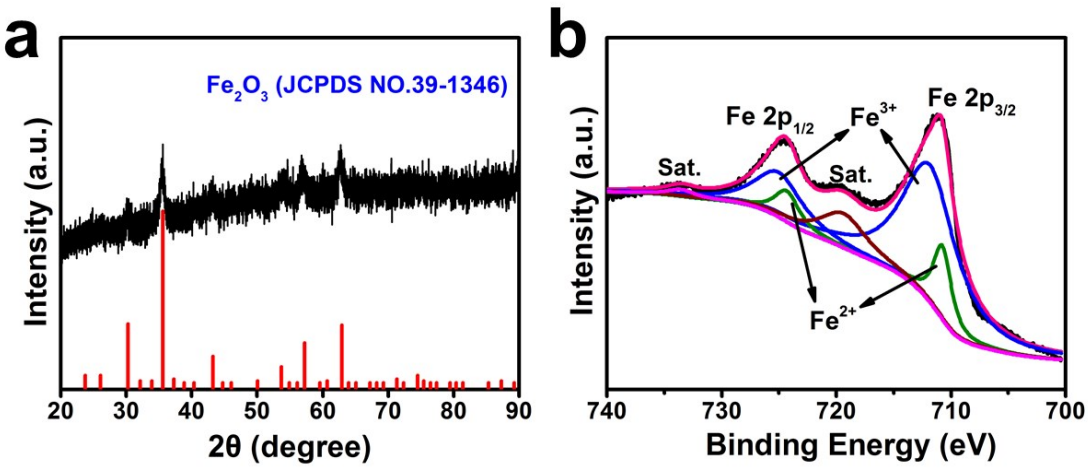

Fig. S11 XRD and XPS characterization of Fe_2O_3/FeS after long-term NRR durability test.

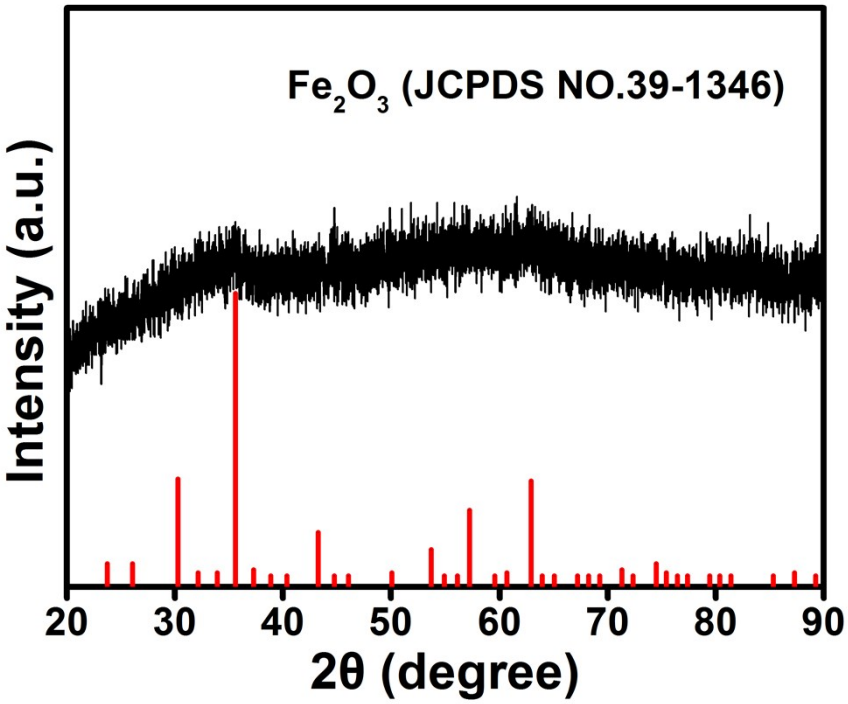

Fig. S12 XRD pattern of Fe_2O_3 product from ChCl/urea DES-assisted approach.

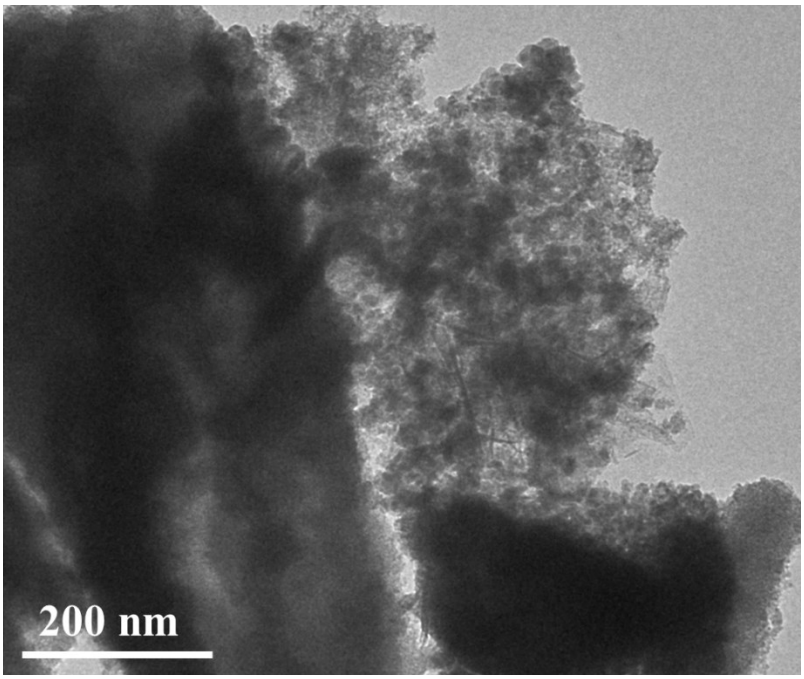

Fig. S13 TEM image of Fe_2O_3 synthesized in ChCl/urea DES.

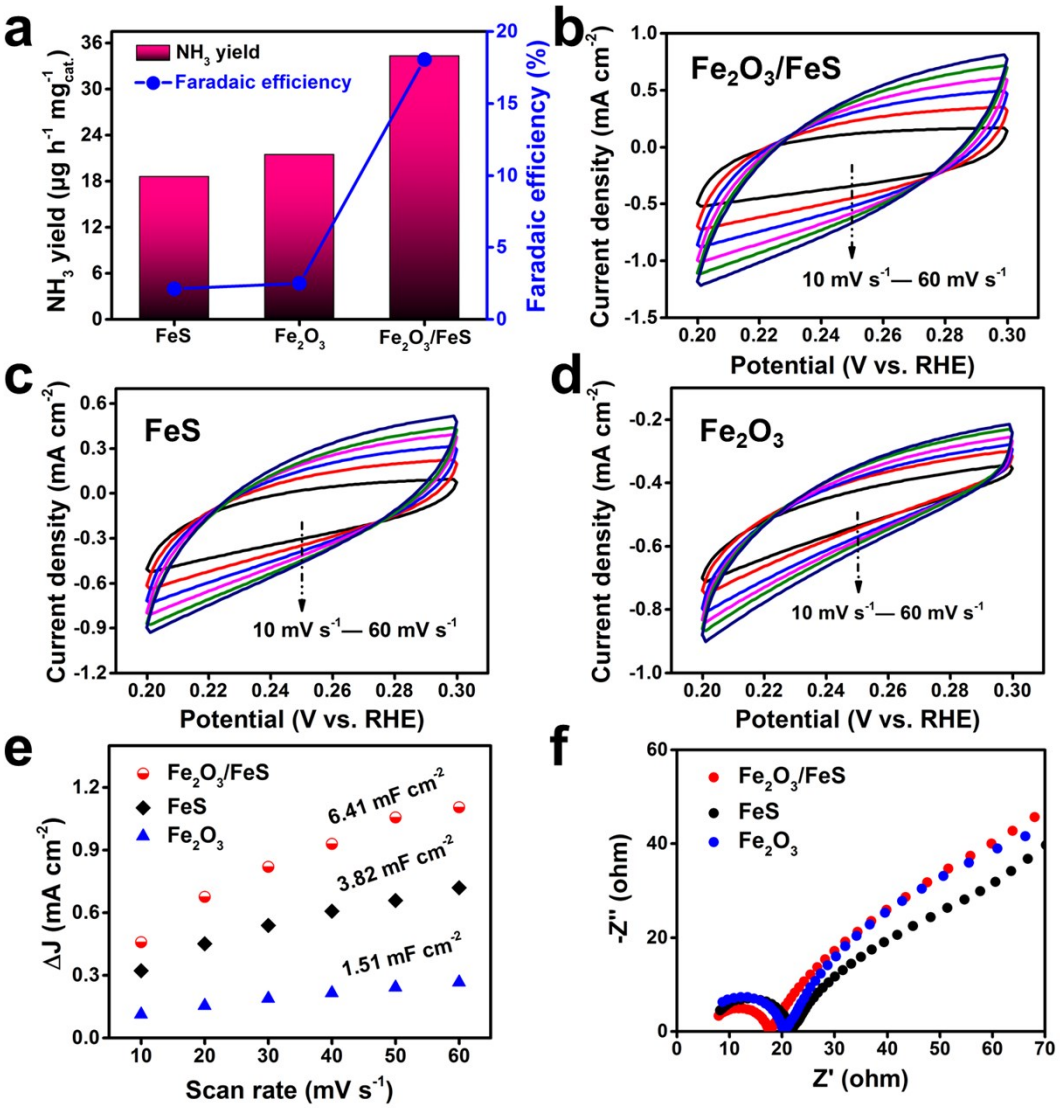

Fig. S14 (a) NH_3 yields and Faradaic efficiencies of the electrocatalysts, (b) CV curves at of Fe_2O_3/FeS, (c) FeS and (d) Fe_2O_3, (e) C_{dl} of Fe_2O_3/FeS, FeS and Fe_2O_3, (f) EIS results of Fe_2O_3/FeS, FeS and Fe_2O_3.

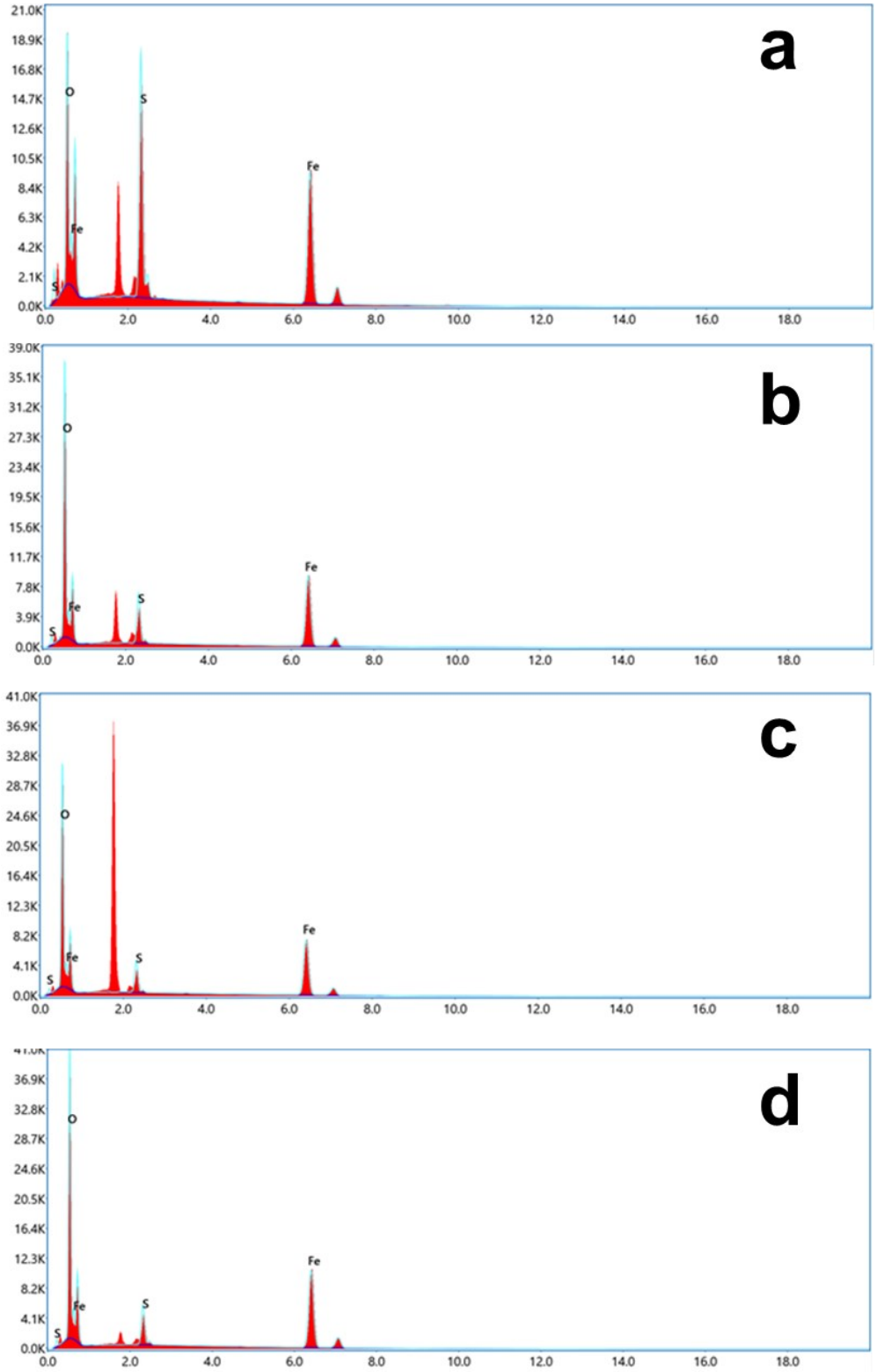

Fig. S15 EDX results of samples with different molar ratio of Fe_2O_3 and FeS prepared by annealing FeS at 400 ^{o}C in air for (a) 1 min, (b) 10 min, (c) 30 min, (d) 1 h. Based on the EDX result, molar ratio of Fe_2O_3 and FeS is 0.46:1, 1.97:1, 2.55:1 and 2.82:1 for (a) 1 min, (b) 10 min, (c) 30 min and (d) 1h.

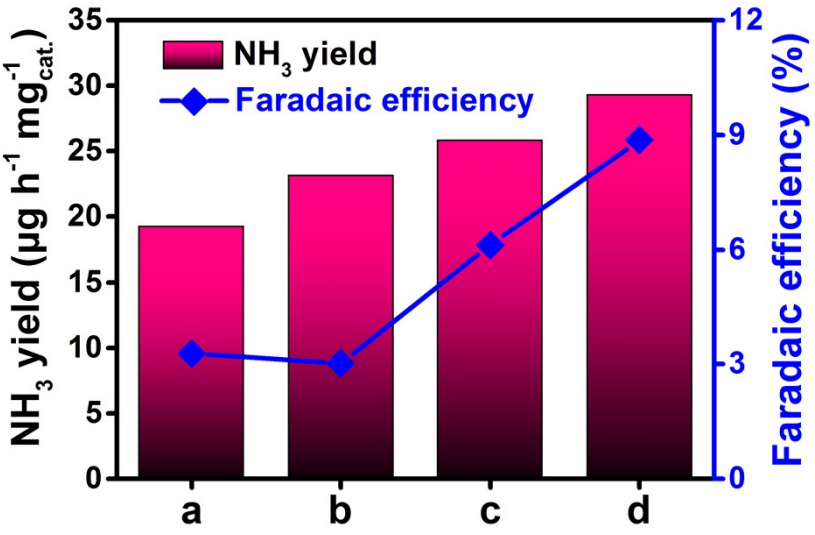

Fig. S16 NH_3 yields and Faradaic efficiencies of samples with different molar ratio of Fe_2O_3 and FeS prepared by annealing FeS at 400 °C in air for (a) 1 min, (b) 10 min, (c) 30 min, (d) 1 h. Molar ratio of Fe_2O_3 and FeS is 0.46:1, 1.97:1, 2.55:1 and 2.82:1 for (a) 1 min, (b) 10 min, (c) 30 min and (d) 1 h.

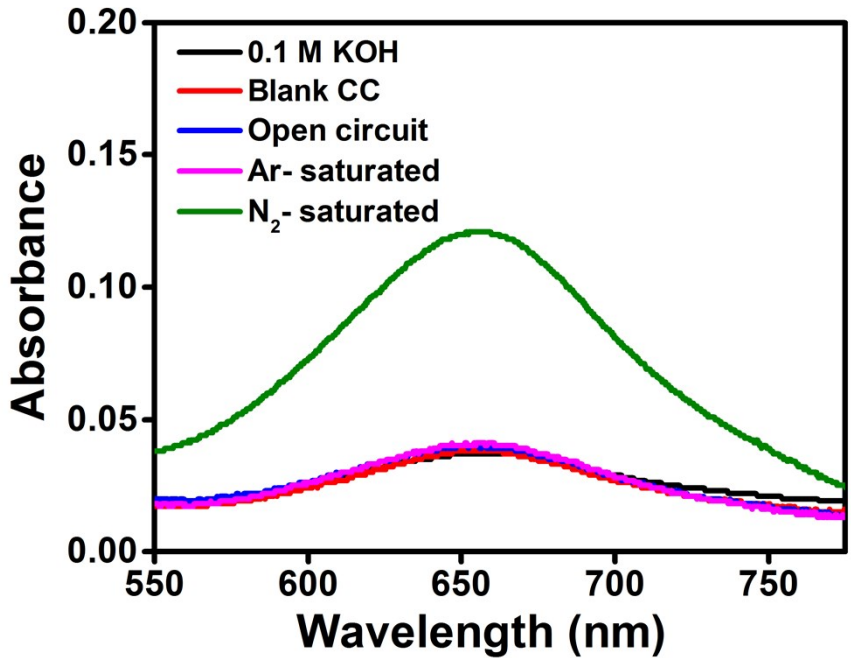

Fig. S17 UV-Vis absorption spectra of the electrolytes from the control experiments (blank carbon cloth used as working electrode, open circuit potential and Ar-saturated

solution) stained with indophenol indicator.

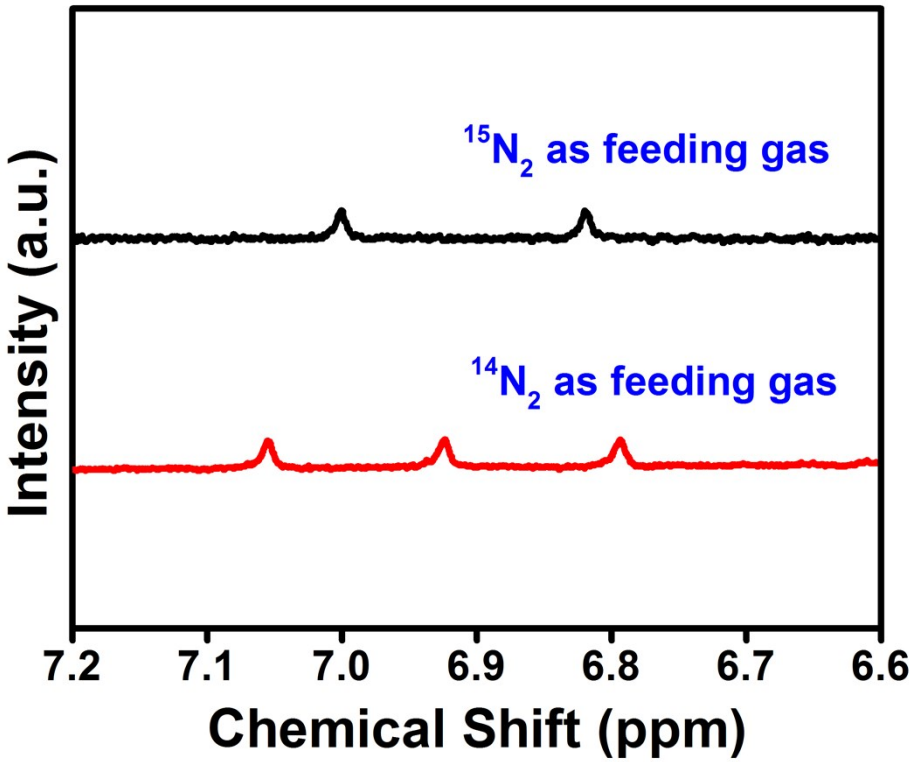

Fig. S18 ^{1}H NMR spectra of the electrolytes under $^{15}N_2$ and $^{14}N_2$ atmosphere.

References

1 A. P. Abbott, G. Capper, D. L. Davies, R. K. Rasheed and V. Tambyrajah, *Chem. Commun.*, 2003, 70-71.

2 P. L. Searle, *Analyst*, 1984, **109**, 549-568.

3 G. W. Watt and J. D. Chrisp, *Anal. Chem.*, 1952, **24**, 2006-2008.

4 Z. Wang, K. Zheng, S. Liu, Z. Dai, Y. Xu, X. Li, H. Wang and L. Wang, *ACS Sustain. Chem. Eng.*, 2019, **7**, 11754-11759.

5 C. Huang, L. Shang, P. Han, Z. Gu, A. M. Al-Enizi, T. M. Almutairi, N. Cao and G. Zheng, *J. Colloid Interf. Sci.*, 2019, **552**, 312-318.

6 X. Xiang, Z. Wang, X. Shi, M. Fan and X. Sun, *ChemCatChem*, 2018, **10**, 4530-4535.

7 H. Du, C. Yang, W. Pu, L. Zeng and J. Gong, *ACS Sustain. Chem. Eng.*, 2020, **8**, 10572-10580.

8 M. Peng, Y. Qiao, M. Luo, M. Wang, S. Chu, Y. Zhao, P. Liu, J. Liu and Y. Tan, *ACS Appl. Mater. Inter.*, 2019, **11**, 40062-40068.

9 J. Zhang, Y. Ji, P. Wang, Q. Shao, Y. Li and X. Huang, *Adv. Funct. Mater.*, 2019, **30**, 1906579.

10 Y. Wang, X. Cui, J. Zhao, G. Jia, L. Gu, Q. Zhang, L. Meng, Z. Shi, L. Zheng, C. Wang, Z. Zhang and W. Zheng, *ACS Catal.*, 2018, **9**, 336-344.

11 X. Xu, X. Tian, B. Sun, Z. Liang, H. Cui, J. Tian and M. Shao, *Appl. Catal. B-Environ.*, 2020, **272**, 118984.

12 C. Wang, J. Gao, J. Zhao, D. Yan and X. Zhu, *Small*, 2020, **16**, 1907091.

13 M. Yuan, H. Zhang, D. Gao, H. He, Y. Sun, P. Lu, S. Dipazir, Q. Li, L. Zhou, S. Li, Z. Liu, J. Yang, Y. Xie, H. Zhao and G. Zhang, *J. Mater. Chem. A*, 2020, **8**, 2691-2700.

14 Z. Ma, J. Chen, D. Luo, T. Thersleff, R. Dronskowski and A. Slabon, *Nanoscale*, 2020, **12**, 19276-19283.

15 C. Lv, C. Yan, G. Chen, Y. Ding, J. Sun, Y. Zhou and G. Yu, *Angew. Chem. Int. Ed.*, 2018, **57**, 6073-6076.

16 Y. Du, C. Jiang, L. Song, B. Gao, H. Gong, W. Xia, L. Sheng, T. Wang and J. He, *Nano Res.*, 2020, 13, 2784-2790.

17 M. Yuan, Q. Li, J. Zhang, J. Wu, T. Zhao, Z. Liu, L. Zhou, H. He, B. Li and G. Zhang, *Adv. Funct. Mater.*, 2020, **30**, 2004208.

18 P. Li, W. Fu, P. Zhuang, Y. Cao, C. Tang, A. B. Watson, P. Dong, J. Shen and M. Ye, *Small*, 2019, **15**, 1902535.